Electoronic structure of twofold-coordinated atoms in silicon-based amorphous semiconductors

Electronic structure of twofold-coordinated atoms in silicon-based amorphous semiconductors

Nobuhiko Ishii
Department of Electrical Engineering, Fukui Institute of Technology, Fukui 910, Japan

Tatsuo Shimizu
Department of Electronics, Faculty of Technology, Kanazawa University, Kanazawa 920, Japan

(Received 1 May 1991; revised manuscript received 1 August 1991)

Electronic states of the twofold-coordinated N atom in a-Si_xNi_{1-x}:H and twofold-coordinated P atom in P-doped a-Si:H have been calculated using the density-functional theory with a local-spin-density approximation. The calculated ^{14}N hyperfine parameters agree fairly well with those observed in N-rich a-Si_xN_{1-x}:H by electron-spin-resonance (ESR) experiments, confirming the ESR center to be a twofold-coordinated N atom. On the other hand, the calculated ^{31}P hyperfine parameters are largely different from the observed values for the ESR center with a 250-G splitting in P-doped a-Si:H. Therefore the ESR center should not be identified as a twofold-coordinated P atom.

I. INTRODUCTION

Electron-spin-resonance (ESR) measurements are useful for the investigation of defect states with unpaired electrons. Especially, the hyperfine structure of the ESR signal as well as the g-value gives us information about the microscopic structure of the defect.

In P-doped a-Si:H the ESR signal with the hyperfine splitting of about 250 G has been observed.[1-6] Although this hyperfine splitting has been attributed to the isotropic hyperfine interaction between an unpaired electron and ^{31}P nucleus ($A_{iso}=250$ G), the microscopic structure of this ESR center is not yet clear. Up to now, three models have been proposed: (1) a neutral fourfold-coordinated P atom,[2] (2) a neutral twofold-coordinated P atom (P_2^0),[3] and (3) a neutral weak Si—P bond between threefold-coordinated Si and P atoms.[6,7]

Recently, Warren, Lenahan, and Curry observed a new ESR signal in N-rich a-Si_xN_{1-x}:H after uv irradiation.[8] From a comparison with a computer analysis of ^{14}N hyperfine interactions, they identified these ESR centers with neutral twofold-coordinated nitrogen atom (N_2^0). ^{14}N hyperfine parameters for this ESR signal were determined as follows: The isotropic hyperfine interaction is $A_{iso}=11\pm1$ G and the anisotropic is $A_{aniso}=12.5\pm1$ G.[8]

If we neglect the spin-polarization effects in the calculation of the hyperfine interaction parameters, the P_2^0 and N_2^0 models for the above-mentioned ESR signals are excluded, because the contribution of the s-type atomic orbitals centered on these twofold-coordinated atoms to the states with an unpaired electron should be very small due to the symmetry,[7] resulting in a very small value of A_{iso}. However, Cook and White pointed out that it is important to take into account the spin-polarization effects in the hyperfine interaction calculation for the Si dangling bond.[9] Accordingly, in order to clarify whether or not the P_2^0 and N_2^0 models are the origins of the above-mentioned ESR signals, it is necessary to calculate the hyperfine interaction by taking into account the spin-polarization effects.

In this paper, we present the results of electronic-structure calculations for the model clusters with P_2^0 and N_2^0, using a first-principles linear combination of atomic orbitals method based on the local-spin-density functional formalism.[10]

II. CALCULATION METHOD AND MODELS

We obtain the electronic structure for the defect model by solving the Kohn-Sham (KS) equation[11] self-consistently,

$$[-\tfrac{1}{2}\Delta+V_\sigma(\mathbf{r})]\Psi_\sigma(\mathbf{r})=E\Psi_\sigma(\mathbf{r}) , \tag{1}$$

where

$$V_\sigma(\mathbf{r})=V_{nucl}(\mathbf{r})+\int\frac{\rho(\mathbf{r}')}{|\mathbf{r}-\mathbf{r}'|}d\mathbf{r}'+V_{xc}^\sigma(\mathbf{r}) . \tag{2}$$

Here σ denotes the spin state, up or down, and the electron density $\rho(\mathbf{r})$ is

$$\rho(\mathbf{r})=\rho_{up}(\mathbf{r})+\rho_{down}(\mathbf{r}) , \tag{3}$$

where

$$\rho_\sigma(\mathbf{r})=\sum_i^{occ}|\Psi_{\sigma i}(\mathbf{r})|^2 . \tag{4}$$

The first and second terms in the right-hand side of Eq. (2) are the Coulomb potentials from nuclei and electrons, respectively. The third one is the exchange-correlation potential which is expressed as the functional of $\rho_{up}(\mathbf{r})$ and $\rho_{down}(\mathbf{r})$. For the $V_{xc}^\sigma(\mathbf{r})$ we have employed the expression by Gunnarsson and Lundqvist.[10]

In order to solve Eq. (1), the KS orbital $\Psi_\sigma(\mathbf{r})$ is represented as a linear combination of atomic orbitals $\varphi_\mu(\mathbf{r})$ as follows:

$$\Psi_\sigma(\mathbf{r})=\sum_\mu C_{\mu\sigma}(\mathbf{r})\varphi_\mu(\mathbf{r}) . \tag{5}$$

Then, we solve the secular equation,

$$|H^{\sigma}_{\mu\nu}-ES_{\mu\nu}|=0 , \tag{6}$$

where $H^{\sigma}_{\mu\nu}$ and $S_{\mu\nu}$ are the Hamiltonian and overlap matrix elements, respectively, between $\varphi_{\mu}(\mathbf{r})$ and $\varphi_{\nu}(\mathbf{r})$. In the present calculation we have employed 1*s* and 2*s* orbitals for the H atom, 1*s*, 2*s*, 2*p*, 3*s*, and 3*p* orbitals for the N atom, and 1*s*, 2*s*, 2*p*, 3*s*, 3*p*, and 3*d* orbitals for the Si and P atoms as $\varphi_{\mu}(\mathbf{r})$.

As a radial part of $\varphi_{\mu}(\mathbf{r})$, we have employed the linear combination of Gaussian-type orbitals (GTO) of the form

$$R_{nl}(r)=r^{l}\sum_{i=1}^{20} c_{nli}e^{-\alpha_i r^2} , \tag{7}$$

where n and l denote the principal and orbital quantum number, respectively, $\alpha_i=0.05\times 2^{i-1}$, and c_{nli} are the coefficients which are obtained by solving the eigenvalue problems of Eq. (1) for free atoms using *s*-, *p*-, and *d*-type GTO's as the basis functions. The eigenvalue problems are solved within the restricted (spin-unpolarized) self-consistent-field (SCF) theory except for the H atom. In these calculations we filled each of the three valence *p* orbitals with one electron in N and P atoms and two-thirds in the Si atom.

In order to solve Eq. (1) self-consistently, the calculations are carried out iteratively as follows: (1) We construct the input charge densities $\rho^{\rm in}_{\sigma}(\mathbf{r})$ by a superposition of the charge densities calculated for free atoms within the restricted SCF theory. (2) The potentials $V^{\rm in}_{\sigma}(\mathbf{r})$ are calculated by Eqs. (2) and (3) for these $\rho^{\rm in}_{\sigma}(\mathbf{r})$. (3) $H^{\sigma}_{\mu\nu}$ and $S_{\mu\nu}$ are calculated. (4) The KS orbitals and eigenvalues are obtained by solving Eq. (6). (5) The charge densities $\rho^{\rm out}_{\sigma}(\mathbf{r})$ are calculated by Eq. (4) using the KS orbitals obtained in step (4). (6) Then step (2) is carried out again by regarding $\rho^{\rm out}_{\sigma}(\mathbf{r})$ as $\rho^{\rm in}_{\sigma}(\mathbf{r})$. If $\rho^{\rm in}_{\sigma}(\mathbf{r})$ and $\rho^{\rm out}_{\sigma}(\mathbf{r})$ satisfy the condition of self-consistency then the calculations are finished.

$\rho^{\rm in}(\mathbf{r})$ and $V^{\rm in}_{\sigma}(\mathbf{r})$ are numerically fitted to the analytic forms [the right-hand sides of Eqs. (8) and (9) discussed below]. 7000–10000 sampling points for the model clusters are used in the calculations. These analytic forms are used in order to calculate the integrals in steps (2) and (3) analytically.

The $\rho(\mathbf{r})$ is numerically fitted to the following form[12] in order to calculate the second term in the right-hand side of Eq. (2) analytically:

$$\rho(\mathbf{r})=\sum_{A,m}\rho_{A,m}e^{-\beta_m|\mathbf{r}-\mathbf{r}_A|^2} . \tag{8}$$

Here, the sum is over all the atoms in the cluster and there are 20–30 GTO's centered on each atom. $\rho_{A,m}$ are the coefficients to be obtained from the fit. Gaussian exponents β_m have been optimized and we have achieved an error in this fit of $\rho(\mathbf{r})$ to less than $\pm 0.1\%$ of the total electrons.

The potential $V_{\sigma}(\mathbf{r})$ calculated by Eq. (2) is numerically fitted to the following form[12] in order to calculate $H^{\sigma}_{\mu\nu}$ analytically:

$$\begin{aligned} V_{\sigma}(\mathbf{r})=&-\sum_{A}\frac{Z_A}{|\mathbf{r}-\mathbf{r}_A|}e^{-\gamma_{A,0}|\mathbf{r}-\mathbf{r}_A|^2} \\ &+\sum_{A,k}v^{\sigma}_{A,k}e^{-\gamma_{A,k}|\mathbf{r}-\mathbf{r}_A|^2} \\ &+\sum_{A',k'}v^{\sigma}_{A',k'}e^{-\eta_{k'}|\mathbf{r}-\mathbf{r}_{A'}|^2} , \end{aligned} \tag{9}$$

where the first and second sums are over GTO's divided by $|\mathbf{r}-\mathbf{r}_A|$ and GTO's centered on all atoms in the cluster, respectively, and the third is over GTO's centered on the auxiliary sites which are introduced in order to reproduce the difference between $V_{\rm up}(\mathbf{r})$ and $V_{\rm down}(\mathbf{r})$ at the neighbor of the defect atom. $v^{\sigma}_{A,k}$ and $v^{\sigma}_{A',k'}$ are the coefficients which are obtained from the fit. For $\gamma_{A,0}$ and $\gamma_{A,k}$ we have employed the values optimized for the potential of a free atom. In addition, the values of $\eta_{k'}$ for each auxiliary site distribute between 0.2 and 7.0. Z_A is the atomic number of the atom A. In the fits we have achieved the rms error of less than 0.4–0.8 eV for the clusters mentioned below.

The isotropic and anisotropic hyperfine interaction parameters for the nucleus X at the sites $\mathbf{r}_X$, a^X and A^X_{ij}, respectively, are calculated from the following formula:[9]

$$a^X=\frac{8\pi}{3}g_e\beta_B g_X\beta_n[\rho_{\rm up}(\mathbf{r}_X)-\rho_{\rm down}(\mathbf{r}_X)] , \tag{10}$$

$$\begin{aligned} A^X_{ij}=&g_e\beta_B g_X\beta_n \\ &\times\int[\rho_{\rm up}(\mathbf{r})-\rho_{\rm down}(\mathbf{r})] \\ &\times\frac{3(r_i-r_{Xi})(r_j-r_{Xj})-\delta_{ij}|\mathbf{r}-\mathbf{r}_X|^2}{|\mathbf{r}-\mathbf{r}_X|^5}d\mathbf{r} , \end{aligned} \tag{11}$$

where g_e is the free-electron g value, β_B and β_n are the Bohr and the nuclear magnetons, $g_X=\mu_X/I_X$, and μ_X and I_X are the magnetic moment and the spin of nucleus X, respectively.

You might think that the rms error (0.4–0.8 eV) in the fit by Eq. (9) is too large. However, the magnitude of $V_{\sigma}(\mathbf{r})$ in the bonding regions is greater than ten times as much as this error. In addition, there is a region where the difference between $V_{\rm up}(\mathbf{r})$ and $V_{\rm down}(\mathbf{r})$ has an amount larger than three times as much as this rms error. In this region, $V_{\sigma}(\mathbf{r})$ are reproduced fairly well by this fit. So we believe that this error is not so large. Furthermore, a^X and A^X_{ij}, calculated using the various sets of the auxiliary sites in the fit by Eq. (9), agree with each other within an error of 20% and 1%, respectively. Accordingly, this method should be reliable enough for the present calculations in which only the difference between $\rho_{\rm up}(\mathbf{r})$ and $\rho_{\rm down}(\mathbf{r})$ plays an important role as shown in Eqs. (10) and (11).

The iterative calculations are finished when the changes of the eigenvalues in Eq. (1) become less than 0.03 eV, which generally corresponds to the changes in $a^{\rm P}$ of less than 0.3 G and $a^{\rm N}$ of less than 0.05 G.

The calculations were carried out for four clusters, PSi_2H_6, PSi_3H_8, NSi_2H_6, and $N_3Si_2H_8$. The atomic configurations for PSi_3H_8 and $N_3Si_2H_8$ clusters are shown

in Figs. 1 and 2, respectively, and Cartesian coordinates of the atoms in these two clusters are listed in Tables I and II. The P atom (number 1 in Fig. 1) and the N atom (number 1 in Fig. 2) are twofold coordinated. The PSi_2H_6 cluster is constructed by removing four atoms (numbers 4, 10, 11, and 12 in Fig. 1) from the PSi_3H_8 cluster and attaching an H atom to the Si atom (number 3 in Fig. 1). Then, this PSi_2H_6 cluster has C_{2v} point-group symmetry. The NSi_2H_6 cluster is constructed from the PSi_2H_6 cluster by substituting the N atom for a P atom without changing all bond angles and with the bond length $d_{Si\text{-}N}=1.74$ Å. In the PSi_2H_6, PSi_3H_8, and NSi_2H_6 clusters, all bond angles are 109.5°. In the $N_3Si_2H_8$ cluster, the bond angles around Si atoms distribute between 105° and 115°, and those around N atoms distribute between 112° and 125°. The bond lengths in these four clusters are as follows: $d_{Si\text{-}Si}=d_{Si\text{-}P}=2.35$ Å, $d_{Si\text{-}N}=1.74$–1.75 Å, $d_{Si\text{-}H}=1.48$ Å, and $d_{N\text{-}H}=1.02$ Å.

III. RESULTS AND DISCUSSION

A. ^{31}P hyperfine interactions

We call the KS orbital which is most strongly localized on the twofold-coordinated atom among the occupied ones the defect KS orbital. The hyperfine interaction parameters calculated for the twofold-coordinated ^{31}P nuclei in the PSi_2H_6 and PSi_3H_8 clusters are shown in Table III. It is found that a^P comes mainly from the valence-polarization effect. In the PSi_3H_8 cluster, the localization of the calculated defect KS orbital on the P_2^0 atom is about 80%. The calculated defect KS orbital is approximately the $3p_z$ orbital on the P_2^0 atom in character due to its symmetry, as pointed out previously.[7] In other words, the mixture of s-type orbitals on the P_2^0 atom into the defect KS orbital is very small. Accordingly the contribution to a^P from the defect KS orbital is small, as shown in Table III(b).

The fact that the contribution to a^P from the defect KS orbital is exactly zero for the PSi_2H_6 cluster is due to the C_{2v} symmetry of its cluster. On the other hand, although this symmetry is broken down in the PSi_3H_8 cluster, a^P does not have a large contribution from the defect KS orbital. The reason is as follows: If we consider only a twofold-coordinated atom and its first-nearest neighbors, this planar molecule has C_s symmetry. As a result, s-type orbitals on the twofold-coordinated atom do not mix into the KS orbitals, which include as a component a $3p$ orbital on that atom perpendicular to the plane constructed by these three atoms. This symmetry may be broken down by the interactions between the twofold-coordinated atom and the atoms beyond its first-nearest neighbors. The breaking of this symmetry is perturbative. Accordingly the mixture of s-type orbitals on the twofold-coordinated atom, into the defect KS orbital which mainly consists of $3p$ orbital on that atom, is always small. So the contribution to the isotropic hyperfine interaction from this defect KS orbital is small.

The calculated a^P corresponds to the observed splitting of the ESR signal in P-doped a-Si:H ($A_{iso}=250$ G).[1–6] However, the calculated values shown in Table III are too small to explain the observed splitting. If the calculations are carried out for larger clusters the results should become somewhat smaller. Accordingly, the P_2^0 model cannot explain the ESR signal with the hyperfine splitting observed in P-doped a-Si:H.

B. ^{14}N hyperfine interactions

The hyperfine interactions calculated for the twofold-coordinated ^{14}N nuclei in the NSi_2H_6 and $N_3Si_2H_8$ clusters are shown in Table IV. The results shown in Table IV are qualitatively equal to those in Table III. In the $N_3Si_2H_8$ cluster, the localization of the calculated defect KS orbital on the N_2^0 atom is about 60%. Since the defect KS orbital mainly consists of a $2p_z$ orbital on an N_2^0 atom due to its symmetry. a^N and A_{ii}^N's are dominated by the contribution from the valence polarization and the defect KS orbital, respectively. In addition, this means that the defect KS orbital has nearly axial symmetry and approximately leads to

$$|A_{xx}^N|=|A_{yy}^N|=A_{zz}^N/2$$

as shown in Table IV(a), which was assumed by Warren, Lenahan, and Curry in their computer analysis of ^{14}N hyperfine interactions.[8] The calculated values of a^N and $|A_{xx}^N|$ shown in Table IV correspond to the observed A_{iso}

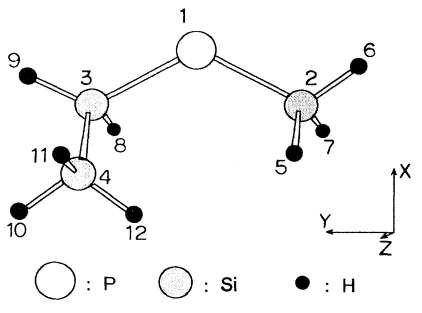

FIG. 1. Atomic configuration for PSi_3H_8 cluster. The P atom is twofold coordinated.

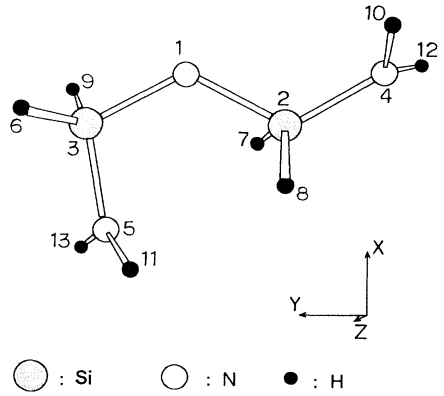

FIG. 2. Atomic configuration for $N_3Si_2H_8$ cluster. The N atom (number 1) is twofold coordinated.

TABLE I. Cartesian coordinates of atoms in the PSi_3H_8 cluster used in the calculations (in units of Å).

No.	Atom	x	y	z	No.	Atom	x	y	z
1	P	0.000	0.000	0.000	7	H	−2.211	−1.919	−1.208
2	Si	−1.357	−1.919	0.000	8	H	−2.211	1.919	−1.208
3	Si	−1.357	1.919	0.000	9	H	−0.502	3.127	0.000
4	Si	−2.713	1.919	1.919	10	H	−3.568	3.127	1.919
5	H	−2.211	−1.919	1.208	11	H	−1.859	1.919	3.127
6	H	−0.502	−3.127	0.000	12	H	−3.568	0.710	1.919

TABLE II. Cartesian coordinates of atoms in the $N_3Si_2H_8$ cluster used in the calculations (in units of Å).

No.	Atom	x	y	z	No.	Atom	x	y	z
1	N	0.000	0.000	0.000	8	H	−1.772	−1.580	1.175
2	Si	−0.874	−1.514	0.000	9	H	−0.521	2.289	−1.211
3	Si	−0.874	1.514	0.000	10	H	0.793	−3.229	0.627
4	N	0.242	−2.847	−0.135	11	H	−3.193	0.929	0.627
5	N	−2.587	1.215	−0.135	12	H	0.163	−3.333	−1.023
6	H	−0.482	2.324	1.175	13	H	−2.968	1.527	−1.023
7	H	−1.721	−1.595	−1.211					

TABLE III. Hyperfine interaction parameters (in units of G) calculated for twofold-coordinated ^{31}P nuclei in PSi_2H_6 and PSi_3H_8. (a) Net values of ^{31}P hyperfine parameters. The experimental values is also shown. (b) Direct and induced contributions to the isotropic hyperfine parameter a^P.

(a)

Cluster	a^P	A^P_{xx}	A^P_{yy}	A^P_{zz}
PSi_2H_6	68.5	−108.3	−106.2	214.5
PSi_3H_8	65.4	−100.9	−100.6	201.5
Experiment[a]	250			

(b)

	PSi_2H_6	PSi_3H_8
Defect KS orbital	0.0	5.9
Valence polarization	88.1	78.8
2s core polarization	−13.7	−13.7
1s core polarization	−5.9	−5.6
net	68.5	65.4

[a]References 1–6.

TABLE IV. Hyperfine interaction parameters (in units of G) calculated for twofold-coordinated ^{14}N nuclei in NSi_2H_6 and $N_3Si_2H_8$. (a) Net values of ^{14}N hyperfine parameters. Experimental values are also shown. (b) Direct and induced contributions to the isotropic hyperfine parameter a^N.

(a)

Cluster	a^N	A^N_{xx}	A^N_{yy}	A^N_{zz}
NSi_2H_6	12.5	−14.1	−14.4	28.5
$N_3Si_2H_8$	13.4	−12.2	−13.2	25.4
Experiment[a]	11±1		$\lvert A^N_{xx}\rvert = \lvert A^N_{yy}\rvert = 12.5\pm1$	

(b)

	NSi_2H_6	$N_3Si_2H_8$
Defect-KS-orbital	0.0	2.6
Valence polarization	16.6	14.6
1s core polarization	−4.1	−3.8
net	12.5	13.4

[a]Reference 8.

(11±1 G) and A_{aniso} (12.5±1 G),[8] respectively. The agreement between the calculated and observed values is fairly good.

The contribution to a^{N} from the spin-polarization effects and A_{ii}^{N}'s shown in Table IV decrease by about 10% in magnitude with the increase in the cluster size. These changes, however, are considerably small in comparison with about a 45% increase of the number of atoms in the cluster. On the other hand, the net value of a^{N} for the $N_3Si_2H_8$ cluster is somewhat larger than that for the NSi_2H_6 cluster. This is due to the increase in the contribution from the defect KS orbital, which originates from the lowering of the symmetry in the $N_3Si_2H_8$ cluster, as mentioned above. Although the calculated results for the clusters larger than $N_3Si_2H_8$ should become somewhat small, the agreement between the calculated and observed results should not be spoiled. Accordingly, we conclude that the origin of the new ESR signal in N-rich a-Si_xN_{1-x}:H, whose intensity increases by uv irradiation,[8] is N_2^0 centers.

However, this conclusion does not necessarily mean that these N_2^0 centers are created from N_2^- centers by uv irradiation. It is possible that in N-rich a-Si_xN_{1-x}:H, N_2^0 centers are created from N_4^+-N_3^0 units by the breaking of the N—N bond due to the capture of an electron.[13,14] Namely,

$$N_4^+\text{-}N_3^0 + \text{electron} \rightarrow N_3^0 + N_2^0 \ . \tag{12}$$

This reaction is reversed by annealing.

This mechanism has been generalized and applied to other cases in amorphous semiconductors.[15] In P-doped a-Si:H, this does not suggest that the P_2^0 centers increase by light soaking, because P_4^+-P_3^0 units should scarcely exist due to a small content of P. In fact, as mentioned above, the results calculated for P_2^0 models cannot explain the ESR signal with hyperfine splitting observed in P-doped a-Si:H before and after light soaking.

IV. CONCLUSIONS

We presented the results of electronic-structure calculations for P_2^0 and N_2^0 models using the density functional theory with a local-spin-density approximation. The ^{14}N hyperfine parameters calculated for N_2^0 models are fairly close to those observed for a new ESR signal in N-rich a-Si_xN_{1-x}:H. Accordingly, it is confirmed that the origin of this ESR signal is N_2^0 centers. On the other hand, the ^{31}P hyperfine parameters calculated for P_2^0 models cannot explain the ESR signal with the hyperfine splitting of 250 G observed in P-doped a-Si:H. It is decisively important to take into account the spin-polarization effects, especially the valence polarization, in the calculations of the isotropic hyperfine interaction parameters for the twofold-coordinated defects.

[1]M. Stutzmann and J. Stuke, J. Non-Cryst. Solids **66**, 145 (1984).
[2]M. Stutzmann and R. A. Street, Phys. Rev. Lett. **54**, 1836 (1985).
[3]I. Hirabayashi, K. Morigaki, S. Yamasaki, and K. Tanaka, in *Optical Effects in Amorphous Semiconductors,* edited by P. C. Taylor and S. G. Bishop, AIP Conf. Proc. No. 120 (AIP, New York, 1984), p. 8.
[4]S. Yamasaki, S. Kuroda, H. Okushi, and K. Tanaka, J. Non-Cryst. Solids **77&78**, 339 (1985).
[5]S. Schutte, F. Finger, and W. Fuhs, J. Non-Cryst. Solids **114**, 411 (1989).
[6]T. Shimizu, X. Xu, T. Ohta, M. Kumeda, and N. Ishii, Solid State Commun. **67**, 941 (1988).
[7]N. Ishii, M. Kumeda, and T. Shimizu, Solid State Commun. **53**, 543 (1985).
[8]W. L. Warren, P. M. Lenahan, and S. E. Curry, Phys. Rev. Lett. **65**, 207 (1990).
[9]M. Cook and C. T. White, Phys. Rev. Lett. **59**, 1741 (1987); Phys. Rev. B **38**, 9674 (1988).
[10]O. Gunnarsson and B. I. Lundqvist, Phys. Rev. B **13**, 4274 (1976); **15**, 6006 (1977).
[11]W. Kohn and L. J. Sham, Phys. Rev. **140**, A1133 (1965).
[12]F. Zandiehnadem and W. Y. Ching, Phys. Rev. B **41**, 12 162 (1990).
[13]N. Ishii, M. Kumeda, and T. Shimizu, Jpn. J. Appl. Phys. **24**, L244 (1985).
[14]D. Redfield and R. H. Bube, Phys. Rev. Lett. **65**, 464 (1990).
[15]T. Shimizu, N. Ishii, and M. Kumeda, in *Tetrahedrally-Bonded Amorphous Semiconductors,* edited by D. Adler and H. Fritzsche (Plenum, New York, 1985), p. 187.